Brittle metallic glass deforms plastically at room temperature in glassy multilayers

Parmanand Sharma,[1,*] Kunio Yubuta,[1] Hisamichi Kimura,[1] and Akihisa Inoue[1,2]
[1]*Institute for Materials Research, Tohoku University, Sendai 980-8577, Japan*
[2]*World Premier Initiative (WPI) Center, Advanced Institute for Materials Research (AIMR), Tohoku University, Sendai 980-8577, Japan*
(Received 5 March 2009; revised manuscript received 4 May 2009; published 7 July 2009)

Bulk metallic glasses are emerging as a new class of materials that can have applications ranging from structural materials to materials for future nanotechnology. However, catastrophic mechanical failure is a serious issue hindering the use of these materials in engineering applications. Here we introduce an approach to understanding and solving the problem of brittleness of metallic glasses. We have shown that even a very brittle metallic glass (La based) can be forced to deform plastically at room temperature if it is made in the form of multilayers involving other metallic glasses, i.e., a two-phase glass. The mechanically soft glassy layer (La based) having a lower critical shear stress acts as a nucleation or an initiation site for shear bands and the mechanically hard glassy layer (Zr based) acts as an obstacle to the propagation of shear bands. This process results in the multiplication of shear bands. Since the shear bands are associated with a local rise in temperature, a large number of shear bands can raise the overall temperature of the soft layer and eventually can drive it to the supercooled liquid state, where deformation of metallic glass is very large and homogeneous. The results reported here not only clarify the mechanism of large plastic deformation in two-phase glassy alloys but also suggest the possibility of a different kind of two-phase bulk glassy alloys exhibiting large plastic deformation at room temperature.

DOI: 10.1103/PhysRevB.80.024106 PACS number(s): 62.20.−x, 62.25.Mn, 68.60.−p

I. INTRODUCTION

Bulk metallic glasses (BMGs) have excellent mechanical, chemical, and functional properties (such as soft magnetism).[1] Many different kinds of BMG systems have been developed and the maximum thickness of some of the Zr- and Pd-based BMGs has reached several centimeters.[2] Two major problems, which limit their applications, are their brittle nature or poor plasticity at room temperature and the lack of proper joining or integration technology. Attempts have been made to improve the plasticity of BMGs. The inhomogeneous microstructures with isolated dendrites or nanocrystalline precipitates in a BMG matrix are shown to stabilize the glass against brittle fracture by formation of multiple shear bands.[3–5] Although such microstructures improve the plastic deformation, they degrade the basic properties of the glass (such as a random structure, isotropic nature, no grains and grain boundaries, etc.).

In monolithic metallic glasses plastic deformation can be enhanced by the introduction of compressive residual stresses.[6] However the introduction of such a stress in the whole volume of the sample is challenging. Recently Liu *et al.*[7] reported a large plastic deformation of ~160% in compression for a monolithic BMG. The authors reported that no phase separation was observed but ion milling of the sample resulted in two different kinds of regions where the milling rate was different. This observation led the authors to conclude that there might be mechanically soft and hard regions in the sample. The existence of huge plasticity was because of this special structure. They explained that the shear transformation zones occur preferentially in the soft regions and evolve into shear bands upon loading. Consequently the propagation of a large number of shear bands formed in the soft regions was impended by the hard regions, resulting in shear-band multiplication. Later on Du *et al.*[8] made a two-phase BMG and observed a large plastic deformation of ~30%. The two phases formed in the BMG were $Zr_{68.5}Cu_{8.1}Ni_{21.3}Al_{2.1}$ and $Zr_{62.4}Cu_{16.7}Ni_{14.6}Al_{6.3}$ with hardness values of ~6.17 and 5.22 GPa, respectively. To explain the existence of large plasticity in this two-phase glassy alloy, an explanation similar to Liu *et al.*[7] was proposed. On careful examination of these reported results, it can be clearly noticed that in both the cases the initial alloy system was Zr-Al-Cu-Ni in which the phase-separated regions have only slight variation in composition and mechanical properties. It is also reported that high Poisson's ratio (ν) of metallic glasses corresponds to good plasticity.[9] The BMGs with $\nu > 0.32$ were shown to exhibit plasticity. ν for Zr-based BMGs is already above this critical value.

In contrast to introducing obstacles to shear-band propagation in a glass, a complete suppression of shear-band nucleation offers another way of enhancing plasticity.[10–13] It was proposed that the deformation of metallic glasses occurs through four sequential stages: formation of a single shear-transformation zone (STZ), formation of STZ clusters, shear-band nucleation, and shear-band propagation.[14] Shear-band nucleation is the rate controlling stage and once a critical nucleus is formed, the shear band propagates catastrophically. The estimated size of the shear-band nucleus is ~20 nm in diameter.[13] If the characteristic dimension of an amorphous phase is less than 10–20 nm, it would be extremely difficult to initiate a localized shear band and thus delay fracture. Based on this concept, multilayered structures (nanolaminates) consisting of a thin amorphous metallic layer (<20 nm) sandwiched between nanocrystalline metals were studied.[10–13] A large tensile ductility was reported in these nanocrystalline-amorphous nanolaminates. Wang *et al.*[11] believed that amorphous-crystalline interfaces are necessary for continuous generation and absorption of dislocations in order to sustain plastic deformation, whereas Nieh and Wadsworth[13] believed that the nanocrystalline metal in a

multilayer has intrinsic plasticity and the role of the interface is to transfer the load. In contrast to the above reports, studies on amorphous crystalline nanolaminates by Zong *et al.*[15] (polycrystalline Ag/amorphous CoZrNb) and Lv *et al.*[16] (polycrystalline Ag/amorphous CoZrNb) showed the existence of shear-band nucleation even in 10-nm-thick amorphous layers. Thus, the role of the glass-crystal interface in improving tensile ductility and plasticity remains controversial.

From the reported literature it appears that multiple shear bandings or the complete suppression of a shear band is effective in the development of room-temperature plastic or ductile BMGs. However the length scale required for suppression of a shear band is less than 20 nm. In the case of two-phase BMGs, the reported length scale of phase-separated regions varies from nanometers to several tens of micrometers.[8,17,18] Therefore, suppression of shear-band formation is unlikely and an alternative way of improving plasticity is through creating sites for shear-band multiplication and/or creating obstacles to shear-band propagation.

The motivation of the present study is to clarify whether the existence of a second glassy phase can make any difference in plastic deformation of BMGs. For this, we planned our experiment in such a way that the two glassy phases have very different mechanical and thermal properties. In addition to this, one of the phases should be very brittle. This choice is especially important because if there is an enhancement in plasticity of composite layered structure, the brittle phase will be deformed uniformly. Development of such an ideal nanocomposite BMG is difficult because of very complex thermodynamics involved in the phase separation and also there is the need of a specific composition to form a glass. The problem can be solved by depositing metallic glasses in thin-film multilayered form. This form of two-phase glassy composite preserves all the basic properties (such as free volume, short-range order, etc.) of the monolithic glasses and also provides an excellent control over their volume fraction and joining interface. This is quite unlike two-phase BMGs where the situation is very complicated because of complex microstructures (e.g., uncertain volume fractions, a random distribution of two phases, and a large variation in their sizes). To our knowledge mechanical properties of completely glassy multilayered structure and the effect of glass-glass interface on the propagation of shear band are not yet reported.

For the present study $Zr_{55}Al_{10}Cu_{30}Ni_5$ (will be referred as Zr based) and $La_{55}Al_{25}Ni_{10}Cu_5Co_5$ (will be referred as La based) metallic glass systems were selected because of their very different mechanical and thermal properties (for Zr-based glass transition temperature T_g=690 K and crystallization temperature T_x=780 K; for La-based T_g=460 K and T_x=550 K).[19,20] Zr- and La-based glassy alloys are also known to be immiscible.[21] These two glassy systems are well studied in the literature and one of them (La based) is known to be very brittle. Moreover, fabrication of a multilayered structure of these alloys will not only offer an insight into the plasticity of two-phase glassy alloys but also sheds some light on joining behavior (i.e., second most important problem of BMGs) of two glassy metals. From an application point of view, both the glasses have a large temperature range of supercooled liquid region ($\Delta T_x \sim 85$ K) that allows easy fabrication of microstructures and nanostructures using a nanoimprinting technique.[22]

II. EXPERIMENTAL

Thin films used in the present work were deposited using rf-magnetron sputtering (ULVAC Technologies, Inc., Japan) technique. The sputtering targets (50 mm in diameter, and 5 mm in thickness, and nominal compositions $\sim Zr_{55}Al_{10}Cu_{30}Ni_5$ and $La_{55}Al_{25}Ni_{10}Cu_5Co_5$) were made by the arc-melting technique. The arc-melting chamber was evacuated to a base pressure of $<10^{-3}$ Pa. Appropriate amount of pure metals were weighed and arc melted under an argon atmosphere in a water-cooled copper die. The sputtering chamber was evacuated to a base pressure of $\sim 6 \times 10^{-6}$ Pa, and high-purity argon gas was introduced to obtain a sputtering gas pressure of 0.4 Pa. The rf power applied to the targets was 100 W. The deposition rates were measured to be 0.84 μm/h for Zr-based and 2.2 μm/h for La-based thin films. The actual compositions of the Zr- and La-based glassy thin films were measured by using an electron-probe microanalysis technique. The crystallographic information of the films was obtained by using a Rigaku (model: RINT-Ultima III) x-ray diffractometer (XRD). A field-emission scanning electron microscope (SEM) (Hitachi) was used to observe the surface morphology of the films. Cross-sectional TEM specimens were cut from the multilayered sample and at first thinned by mechanical polishing. The final thinning was done by Ar ions. High-resolution transmission electron microscopy (TEM) was performed by a 200 kV electron microscope (JEOL JEM-2010) having a resolution of 0.19 nm. High-angle annular dark-field scanning transmission electron microscopy (HAADF-STEM) images were taken by a 300 kV electron microscope (FEI Titan 80–300) equipped with a field-emission gun in the scanning transmission electron microscopy mode. In HAADF-STEM observations, a beam probe with a half width of less than 0.2 nm was scanned on samples. The micrometer size pillars were machined by a focused ion-beam (FIB) technique with a Ga ion source (Hitachi, FB-2100). The mechanical testing was carried out by using a nanoindentation technique (Ubi 1, nanomechanical test instrument, Hysitron, Inc. USA). The hardness (H) and the reduced elastic modulus (E_r) were obtained from the load-displacement curve. The indenter tip was used as a scanning probe at a fixed contact load of ~ 0.6 μN in order to acquire a contact mode topographic image of the surface. The acquired image is used to position the indenter at the required location very precisely. For indentation tests on pillars, the indenter was positioned at the center of the pillar (i.e., on axis loading). Microcompression tests were performed with a constant loading rate of 50 μN/s.

III. RESULTS AND DISCUSSION

Individual Zr- and La-based glassy thin films and their multilayers were deposited on (100) silicon substrate by using magnetron sputtering technique. A slight variation

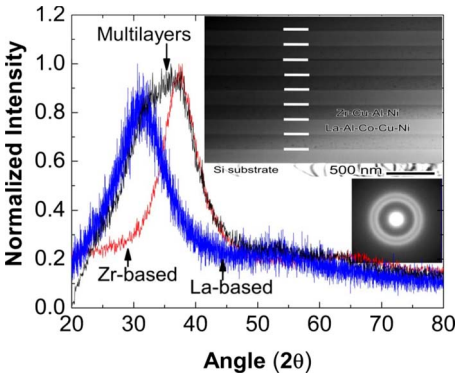

FIG. 1. (Color online) X-ray diffraction curves for La-based, Zr-based glassy thin films, and their multilayered structure. The insets show the cross-sectional transmission electron microscope image and the selected area electron-diffraction (SAED) pattern of the multilayered structure.

in actual film composition ($Zr_{48}Al_{16}Cu_{27}Ni_9$ and $La_{47}Al_{26}Ni_{13}Cu_8Co_6$) and the nominal sputtering target composition ($Zr_{55}Al_{10}Cu_{30}Ni_5$ and $La_{55}Al_{25}Ni_{10}Cu_5Co_5$) was observed. This is common for films deposited with a multielement sputtering target.[23,24]

A. Structural characterization

Figure 1 shows the x-ray diffraction patterns for the individual Zr- and La-based glassy thin films along with a multilayered structure in which each layer thickness is ~200 nm and the total thickness of the films is ~2 μm. The existence of a broad peak is characteristic of a glassy phase. In the case of multilayers, XRD showed two superimposed broad peaks and their 2θ positions exactly correspond to the individual glassy films. Similar XRD pattern was also obtained for the multilayered film in which each layer thickness was ~100 nm. Cross-sectional TEM image shown as an inset in Fig. 1 for the multilayered film with each layer thickness of ~200 nm exhibits a well-defined layered structure with a uniform bilayer period. Two halo rings were observed in the electron-diffraction pattern (inset of Fig. 1) which originate from the individual Zr- and La-based films in the multilayered structure and are consistent with the XRD measurements. Cross-sectional TEM and XRD results proved that the individual Zr- and La-based thin films and their multilayered structure are in a glassy state.

High-resolution transmission electron microscopy images obtained from various sites at the interface prove that the interface is free from nanocrystalline precipitates, and there is no visual difference in the atomic arrangement at the interface compared to the individual layers [Fig. 2(a)]. HAADF-STEM, which is also known as *Z*-contrast imaging is a powerful method to visualize the changes in atomic composition down to atomic level. The HAADF-STEM images [Fig. 2(b)] clearly indicate that the interface between the Zr- and La-based glassy films is very sharp, and there is no interlayer diffusion. The sharpness of the interface was again confirmed from the elemental mapping [Figs. 2(c)–2(e)]. The XRD and the TEM results proved that the multilayered structure is similar to an ideal lamellar two-phase nanocomposite metallic glass.

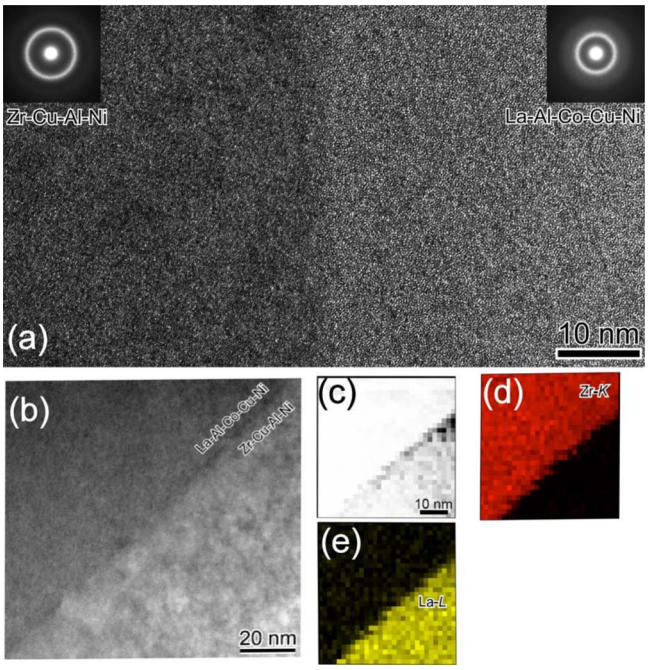

FIG. 2. (Color online) (a) Cross-sectional high-resolution TEM image of multilayered film along with SAED patterns, (b) HAADF-STEM obtained from the interface of Zr- and La-based glassy layers, and (c) TEM image and the corresponding elemental mapping for (d) Zr and (e) La. This figure shows that the interface between the Zr- and the La-based glassy layers is atomically sharp.

B. Mechanical properties

Mechanical properties of individual Zr- and La-based glassy metal thin films and their multilayered structure were investigated by the nanoindentation technique. The experiments were carried out on films with a thickness ranging from 1 to 5 μm for the individual Zr- and La-based glassy thin films and 2 μm for the multilayered structure. The H and the E_r values obtained are 6.6 ± 0.3 GPa and 114 ± 11 GPa, respectively for Zr-based, 3.3 ± 0.2 GPa and 67 ± 7 GPa, respectively, for La based, and 4.4 ± 0.2 GPa and 76 ± 8 GPa, respectively, for multilayered structure. The glassy metal multilayers do not display hardness enhancement similar to crystalline multilayers because of their significantly different deformation mechanism. Hardness of multilayered system can be defined by the isostress and isostrain rule of mixtures,[25]

$$H_{isostress} = \left[\frac{1}{2}\left(\frac{1}{H_A}\right) + \left(\frac{1}{H_B}\right)\right]^{-1}, \quad H_{isostrain} = \frac{1}{2}[H_A + H_B], \tag{1}$$

where H_A and H_B are the hardness of two different layers. The isostress condition assumes that all components of the sample experience the same stress, while the isostrain condition assumes that the each component experiences the same strain. The multilayered films in our indentation experiments

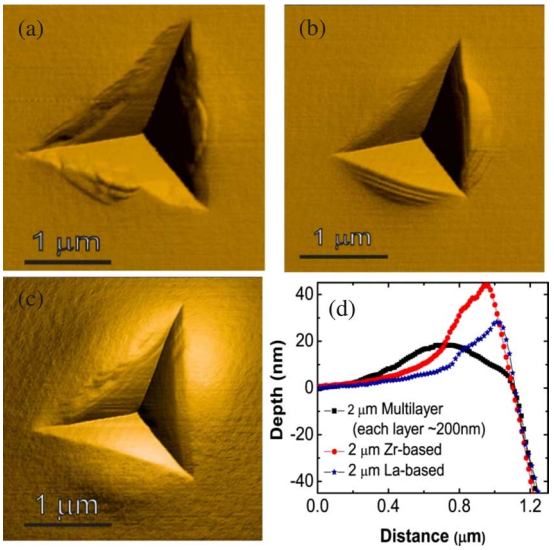

FIG. 3. (Color online) Scanning probe microscope images of the impressions made on (a) La-based, (b) Zr-based, and (c) multilayered glassy thin films. (d) The line profiles obtained in Figs. 3(a)–3(c), showing pileup of material around the indents.

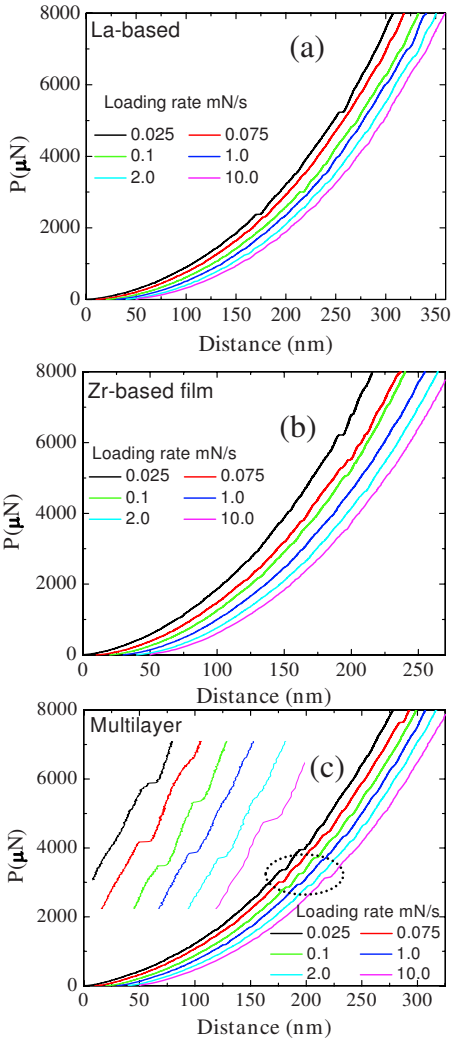

FIG. 4. (Color online) Load displacement curves obtained at different loading rates for (a) La-based, (b) Zr- based, and (c) multilayered glassy thin film. For clarity, these curves are shifted along the *x*-axis.

were oriented in a way expected for the isostress condition. By using the experimentally measured value of hardness using the rule of mixtures for Zr- and La-based glassy metal thin films, the calculated value of hardness for the multilayered structure is 4.4 GPa, which is exactly the same as we have measured for the multilayered structure.

Figure 3 shows the scanning probe microscope (SPM) images of the impressions made by an indent on the film surface (maximum applied load of ~8000 μN). Circular patterns around the indents can be noticed in case of La- and Zr-based metallic glass thin films [Figs. 3(a) and 3(b)]. However, such patterns are absent for multilayered structure [Fig. 3(c)]. The cross-sectional line profile of Figs. 3(a)–3(c) clarify that the features around the indents [Figs. 3(a) and 3(b)] are not cracks but represent overlapping layers of displaced material, i.e., "pileup" [Fig. 3(d)]. The pileup was also observed in the case of multilayered structure, but it was more spread out around the indent, indicating the possibility of more uniform plastic flow of the material. The ability of metallic glasses to deform plastically is dependent on the nucleation and multiplication of shear bands during deformation. In nanoindentation experiments, displacement bursts or pop-ins in the load-displacement curve were associated with the product of rapid strain accommodation of shear bands emitted discretely in sequence.[26] Relatively, a large number of pop-in events can be noticed in the case of La-based glassy thin films compared to Zr-based thin films (Fig. 4). This observation is in contrast to data shown in Fig. 3, where plastic deformation seems to be most pronounced in case of the multilayered and Zr-based thin film.

In order to clarify these symptoms of enhanced plasticity in case of the multilayered structure, we fabricated pillars of diameters 1–4 μm by using a focused ion-beam technique. The typical shape of micropillars is shown in Fig. 5. In SEM images, we could not observe different contrast originating from different types (La or Zr) of glassy layers present in multilayered thin film. Nanoindentation experiments were performed under similar test conditions on micropillars made from Zr, La, and their multilayers, so that they can be easily compared. A sharp Berkovich-type indenter was used instead of a flat punch, typically used in conventional microcompression tests[27,28] because of the following reasons: (1) the present equipment is equipped with a scanning probe microscope that allows easy and very accurate positioning of the indenter[29] and (2) for sharp indenter, the stress intensity at its tip will be higher than what would be achieved with a flat punch. Hence if the test material is brittle, it is more likely to shatter on indenting with a sharp tip. Figure 6 shows the scanning electron microscope image of deformed ~1.5 μm diameter pillars fabricated from La- and Zr-based glassy films and their multilayers. A large amount of plastic deformation can be noticed clearly in the case of multilayered structure. Similar results were also obtained for the compression tests performed on the pillars of diameter 2.0 μm (Fig.

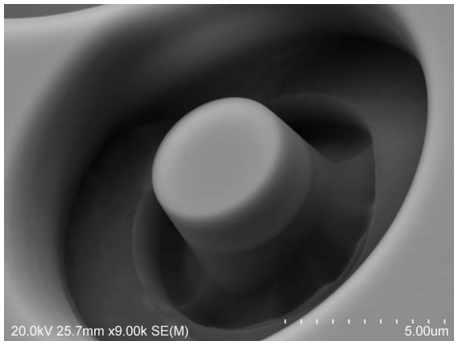

FIG. 5. Typical SEM image of a pillar fabricated by FIB technique on Zr- and La-based multilayered glassy film. The side view of the fabricated pillar is featureless and it is hard to see any contrast in SEM image originating from Zr- and La-based glassy thin-film layers. Similar featureless surface topography was observed for the pillar fabricated from monolithic Zr- and La-based glassy thin films.

7). Although it is a direct comparison of enhanced plasticity, it is worth mentioning that plastic deformation in metallic glasses is known to be dependent on the size of the test specimen.[27,30,31] In compression tests, large plasticity is observed if the aspect ratio is <1 or the specimen size is less than the plastic zone size (r_p).[32] In the present case aspect ratio is more than 1 (~ 1.5). The diameter of the test pillar lies in the plastic zone size (r_p) for Zr-based thin film ($r_p > 50$ μm) but for La-based it is more than r_p (~ 1.3 μm).[33] Moreover, the high-resolution SEM images of the deformed pillars (4–1.5 μm diameter) showed microcracking only in case of La-based glassy thin films (Fig. 8). These results indicate that even a brittle La-based glassy metal deforms plastically in the multilayered structure.

C. Mechanism of large plastic deformation at room temperature in multilayers

Here we will shed some light on the mechanism of enhanced plasticity in the case of multilayered glassy film. The compressive plasticity of BMGs is known to increase monotonically with decreasing aspect ratio.[32] Low plasticity ($<5\%$) is observed for aspect ratio >1 and a high plasticity ($>18\%$) is observed for aspect ratio <1. The aspect ratio plays a more important role in plasticity than the yield strength. In the present case, the total aspect ratio (~ 1.5) of the pillar in multilayered structure is >1, but the individual layers (Zr based or La based), the aspect ratio is <1. Therefore, it is easy to understand that the La-based glassy layer with an aspect ratio <1 will deform uniformly. However this is not the case in present study because the experiments performed under similar test conditions on individual Zr- and La- based glassy thin-film pillars of diameters 1–4 μm, i.e., of aspect ratio 2–0.5, showed a pronounced microscale cracking only in case of La-based glassy thin film. This difference in behavior is basically due to the test geometry. In normal compression tests the application of the load is uniform throughout the test sample, whereas in the present experiments the load is concentrated under a sharp indenter tip.

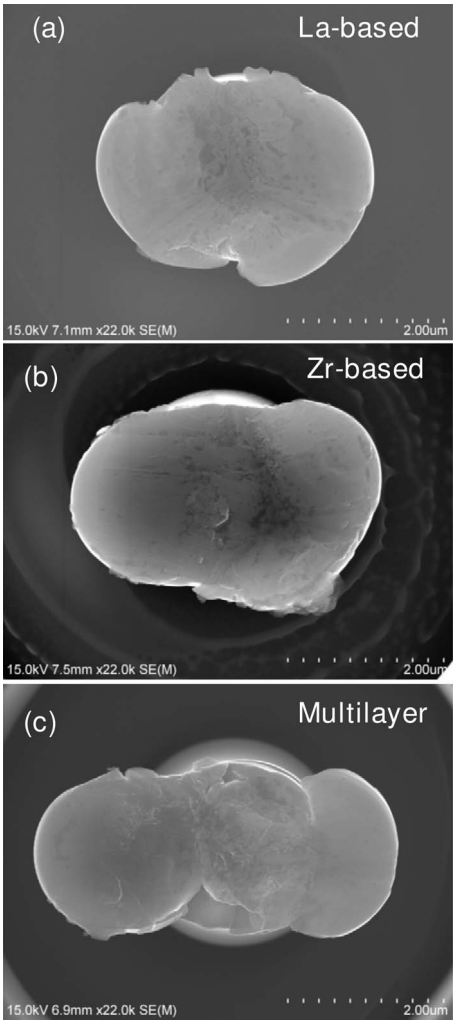

FIG. 6. SEM images of (a) La-based, (b) Zr-based, and (c) multilayered glassy thin-film (1.5 μm diameter) pillars deformed after the microcompression tests performed under identical conditions using a Berkovich-type indenter.

Effectively, the area for loading (apex of the tip diameter <50 nm) is much smaller than the test pillar diameter. Moreover the loading axis in the present case is multiaxial and the shear bands propagating in the directions except normal to the loading axis are more likely to pass throughout the test specimen. In other words, if the test specimen is brittle, it is more likely to shatter in the present test geometry. Therefore a small aspect ratio is not only the cause for enhanced plasticity.

We have noted that the Zr-based and La-based glassy films have a large difference in their mechanical and thermal properties. When the multilayered film is deformed, shear band nucleation starts at first in La-based glassy layer. Since the yield stress for Zr-based glass is almost double than the La-based glass, any shear bands that originate in the La-based glassy layer are unlikely to propagate into the Zr-based glassy layer. This results in multiplication of shear band and accumulation of large amount of stress in the La-based layer. As the load increases, a critical point is reached and the accumulated stress is released by forming shear bands in the

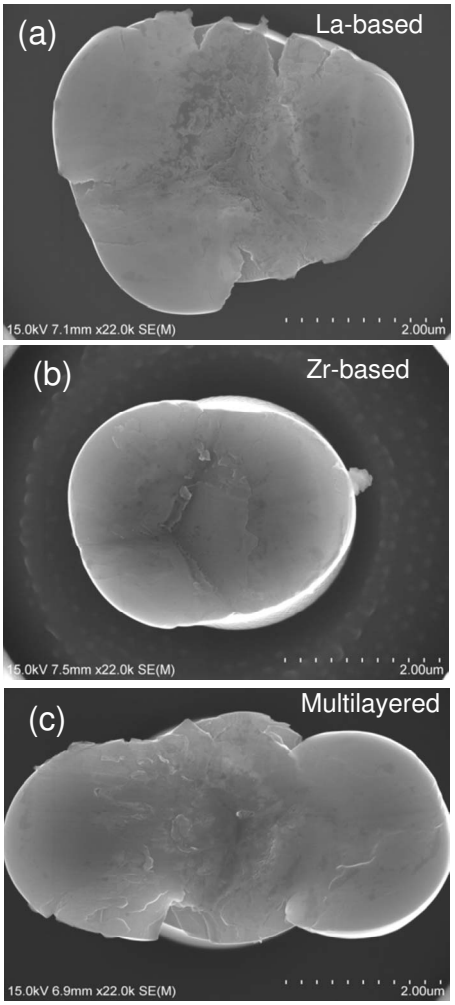

FIG. 7. SEM image of deformed pillars of diameter ~2 μm. (a) La-based, (b) Zr- based, and (c) multilayer. Figures show large deformation in case of multilayered glassy thin film.

harder Zr-based layers. Experimental evidence for this explanation can be noticed from the nanoindentation traces recorded at different loading rates (Fig. 4). Monolithic films showed irregular appearance of pop-in events in the loading curves with respect to the loading rate. In accordance with reported literature pop-in events are more pronounced at low loading rates.[34] However, in the case of multilayered sample, the first noticeable pop-in event is well defined and is almost independent of the loading rate [Fig. 4(c) inset]. We observed this pop-in event at similar loads and depths in all our experiments on multilayered samples. It is also worth to point out that very fine pop-in events can be noticed before this first pronounced pop in but their appearance in the loading curve is random.

The most convincing way to show the multiplication of shear bands in a multilayered sample is to have evidence from SEM and SPM images. However it is hard to observe them from the impressions made by nanoindentation. It is reported that scratching is a more severe deformation mode than indentation for the same normal load. Scratching can produce a large number of shear bands in a same material for which indentation experiment showed no observable shear

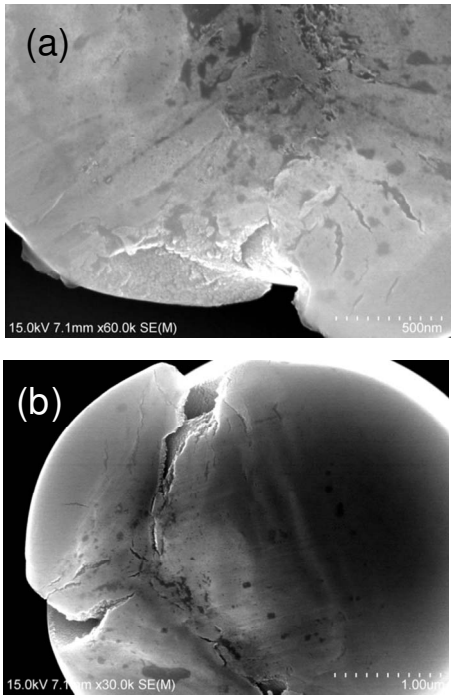

FIG. 8. SEM image of deformed pillars of diameters (a) 1.5 and (b) 3.0 μm fabricated from La-based glassy film. In case of (a) loading of the indenter is in the center of the pillar and it is the magnified image of Fig. 6(a), whereas for (b) the loading was off centered. In both the cases pronounced cracking can be noticed.

bands.[35] Therefore we have also performed scratching experiments on all the three samples under identical conditions and visualized them by using a high-resolution SEM. A pronounced cracking (micron-to-nanometer length scale) was observed in case of La-based glassy film [Fig. 9(a)]. A large number of shear bands similar to the reported literature on Zr-based BMG were observed for the Zr-based thin film [Fig. 9(b)]. Very fine multiple shear bands along with shear bands similar to Zr-based thin film were observed in the multilayered sample [Fig. 9(c)].

The formation of shear band in metallic glasses also raises the temperature within the shear band.[36] This means that a large number of shear bands formed in the La-based glassy layer during deformation of the multilayered structure can raise the overall temperature of the La-based layer. Since the La-based glass has a low T_g (~187 °C), this rise in temperature can eventually drive it into the supercooled liquid temperature range where metallic glasses are known to deform superplastically. In addition to shear-band multiplication, we believe that the low T_g of the La-based glassy layer is also contributing to the overall plastic deformation of the multilayered glassy thin film. The experimental evidence for this explanation can be seen in some of our experiments where the loading of the indenter on the micrometer sized pillar was not exactly at the center. The flowed material was seen at the side of the pillars after the microcompression tests. Fortunately, in some of the SEM images [Fig. 10(a)] we were also able to see different contrasts originating from different layers. On careful examination of Fig. 10(a) it can be noticed that the flowed material after compression testing originates

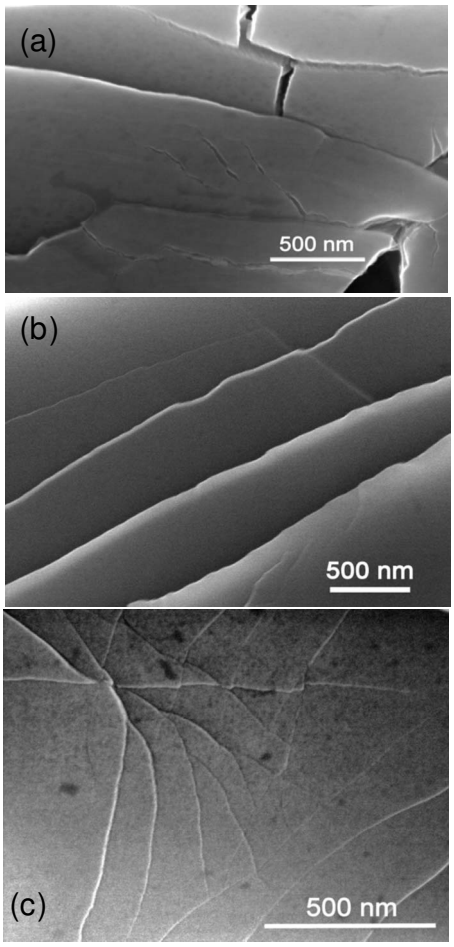

FIG. 9. SEM images of shear bands formed after scratching on (a) La-based, (b) Zr-based, and (c) multilayered glassy thin films. Multiple shear bands can be noticed in case of the multilayered glassy film.

from the second layer from the top, which is exactly the La-based glassy layer according to the deposition geometry. Few more evidences of rise in temperature because of multiple shear banding were also noticed in the side view SEM images of the broken pillar. Figure 10(b) shows the SEM image of a broken pillar fabricated from the multilayered glassy thin film after improper loading in microcompression test. Investigations on this broken pillar reveal very fine globular type features on the side of the pillar [Fig. 10(b)] and vein type structure at the fractured surface. The features observed on the side of the pillar are very different compared to the monolithic glass, where shear bands similar to bulk were observed.[27,28]

Our systematic and detailed experimental results of multilayered glassy thin films clearly suggested that there is a possibility to develop a different kind of BMG that can have large plastic deformation at room temperature. Such type of BMGs should be made up of two glassy phases (mechanical hard and soft phases) and one of the phase that is soft phase should have low value of T_g. The results reported by Kundig *et al.*[37] on La-Zr-Al-Cu-Ni alloy that showed phase separation during quenching from the melt into (La-Cu)- and (Zr-Ni)-rich glassy phases with composition close to those of

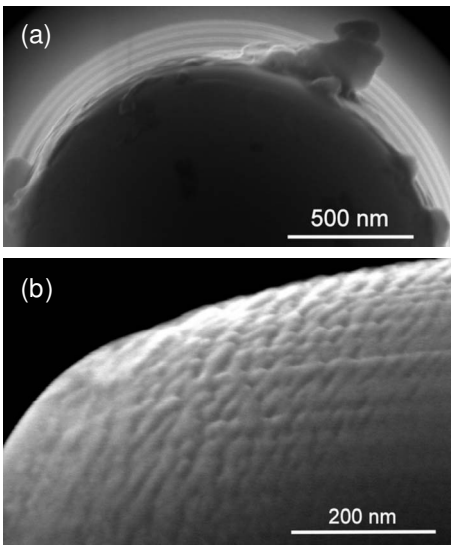

FIG. 10. (a) SEM image of the micropillar after off-axis microcompression testing, sometimes flowed material is observed on the sides of the pillar made from multilayered glassy thin films and (b) SEM image of broken pillar fabricated from multilayered glassy thin film after improper loading in microcompression test. The features observed on the side of the pillar are very different compared to the monolithic glass, where shear bands similar to bulk were observed.

Zr-Ni-Al and La-Cu-Al bulk metallic glasses enhance the possibility of fabrication of these BMGs. Their as-quenched ribbon samples consist of two amorphous phases in spherical shape with a wider range of length scale. In addition to amorphous phases, crystalline phase was also detected in the La-rich areas. Mechanical properties of this two-phase alloyed ribbon were not reported. We believe that further optimization of processing parameters can lead to the development of two-phase (Zr and La based) BMG in this alloy system because both the phases have good glass forming ability along with a strong immiscibility between the Zr and the La elements.

IV. CONCLUSIONS

In summary, Zr- and La-based glassy films and their multilayers were deposited on a silicon substrate in order to understand the enhanced plastic deformation in two-phase bulk glassy alloys. The films obtained were completely glassy without any trace of nanocrystallinity. The interface between Zr- and La-based glassy films is found to be atomically sharp. The multilayered glassy films do not exhibit a hardness enhancement unlike crystalline multilayers. The hardness value of the multilayered glassy alloys lies in between their individual layers. Enhanced plastic deformation was observed for the multilayered glassy thin films as compared to their each individual glassy layer. The reason for the enhanced plasticity was identified. The mechanically soft layer (La based) has a lower critical shear stress for activation of shear bands and serves as a nucleation site for the generation of shear bands. These shear bands find difficulty in entering

the Zr-based layer because of its high critical shear stress. This process causes shear-band multiplication and eventually raises the temperature of the La-based layer to its supercooled liquid range. Improved plastic deformation and atomically sharp interface along with good mechanical properties of the multilayered structure are very important for the fabrication of future micrometer- and nanometer-scale devices. The present experiments also suggest the possibility of fabricating a different kind of two-phase BMGs where one of the phases has a lower T_g and lower mechanical hardness compared to the other glassy phase. Such BMGs will have all the features of a pure glass and are expected to show large plastic deformation at room temperature.

ACKNOWLEDGMENTS

The work was supported by the Development Project on Advanced Metallic Glasses, Inorganic Materials and Joining Technology from The Ministry of Education, Culture, Sports, Science and Technology (MEXT) of Japan. One of the authors (P.S.) would like to thank Shantanu Madge for the fruitful discussion on mechanical properties of bulk metallic glasses.

*Corresponding author; sharmap@imr.tohoku.ac.jp

[1] A. Inoue, Acta Mater. **48**, 279 (2000).
[2] A. Inoue and N. Nishiyama, MRS Bull. **32**, 651 (2007).
[3] C. Fan and A. Inoue, Appl. Phys. Lett. **77**, 46 (2000).
[4] C. C. Hays, C. P. Kim, and W. L. Johnson, Phys. Rev. Lett. **84**, 2901 (2000).
[5] D. C. Hofmann, J. Y. Suh, A. Wiest, G. Duan, M. Lind, M. D. Demetriou, and W. L. Johnson, Nature (London) **451**, 1085 (2008).
[6] Y. Zhang, W. H. Wang, and A. L. Greer, Nature Mater. **5**, 857 (2006).
[7] Y. H. Liu, G. Wang, R. J. Wang, D. Q. Zhao, M. X. Pan, and W. H. Wang, Science **315**, 1385 (2007).
[8] X. H. Du, J. C. Huang, K. C. Hsieh, Y. H. Lai, H. M. Chen, J. S. C. Jang, and P. K. Liaw, Appl. Phys. Lett. **91**, 131901 (2007).
[9] Y. Liu, H. Wu, C. T. Liu, Z. Zhang, and V. Keppens, Appl. Phys. Lett. **93**, 151915 (2008).
[10] T. G. Nieh, T. W. Barbee, and J. Wadsworth, Scr. Mater. **41**, 929 (1999).
[11] Y. Wang, J. Li, A. V. Hamza, and T. W. Barbee, Proc. Natl. Acad. Sci. U.S.A. **104**, 11155 (2007).
[12] A. Donohue, F. Spaepen, R. G. Hoagland, and A. Misra, Appl. Phys. Lett. **91**, 241905 (2007).
[13] T. G. Nieh and J. Wadsworth, Intermetallics **16**, 1156 (2008).
[14] C. A. Schuh, A. C. Lund, and T. G. Nieh, Acta. Mater. **52**, 5879 (2004).
[15] R. L. Zong, S. P. Wen, F. Zeng, Y. Gao, X. W. Li, B. He, and F. Pan, Surf. Coat. Technol. **201**, 7932 (2007).
[16] F. Lv, S. P. Wen, R. L. Zong, F. Zeng, Y. Gao, and F. Pan, Surf. Coat. Technol. **202**, 3239 (2008).
[17] A. Concustell, N. Mattern, H. Wendrock, U. Kuehn, A. Gebert, J. Eckert, A. L. Greer, J. Sort, M. D. Baro, and Scr. Mater. **56**, 85 (2007).
[18] N. Mattern, U. Kuhn, A. Gebert, T. Gemming, M. Zinkevich, H. Wendrock, and L. Schultz, Scr. Mater. **53**, 271 (2005).
[19] A. Inoue and T. Zhang, Mater. Trans., JIM **37**, 185 (1996).
[20] A. Inoue, T. Nakamura, T. Sugita, T. Zhang, and T. Masumoto, Mater. Trans., JIM **34**, 351 (1993).
[21] A. H. Daane and F. H. Spedding, in *Binary Alloy Phase Diagrams*, 2nd ed., edited by T. B. Massalski, H. Okamoto, P. R. Subramanian, and L. Kacprzak (ASM International, The Materials Information Society, Metals Park, OH, 1990), Vol. 3, p. 2444.
[22] P. Sharma, N. Kaushik, H. Kimura, Y. Saotome, and A. Inoue, Nanotechnology **18**, 035302 (2007).
[23] F. X. Liu, Y. F. Gao, and P. K. Liaw, Metall. Mater. Trans. A **39**, 1862 (2008).
[24] P. Sharma, H. Kimura, A. Inoue, E. Arenholz, and J.-H. Guo, Phys. Rev. B **73**, 052401 (2006).
[25] J. B. Vella, A. B. Mann, H. Kung, C. L. Chien, T. P. Weihs, and R. C. Cammarata, J. Mater. Res. **19**, 1840 (2004).
[26] C. A. Schuh and T. G. Nieh, J. Mater. Res. **19**, 46 (2004).
[27] Y. H. Lai, C. Lee, Y. Cheng, H. Chou, H. Chen, X. Du, C. Chang, J. Huang, S. Jian, and J. Jang, Scr. Mater. **58**, 890 (2008).
[28] B. E. Schuster, Q. Wei, T. C. Hufnagel, and K. T. Ramesh, Acta Mater. **56**, 5091 (2008).
[29] Jose M. San Juan, M. L. Nó, and C. A. Schuh, Adv. Mater. **20**, 272 (2008).
[30] W. F. Wu, Z. Han, and Y. Li, Appl. Phys. Lett. **93**, 061908 (2008).
[31] H. Guo, P. F. Yan, Y. B. Wang, J. Tan, Z. F. Zhang, M. L. Sui, and E. Ma, Nature Mater. **6**, 735 (2007).
[32] Z. F. Zhang, H. Zhang, X. F. Pan, J. Das, and J. Eckert, Philos. Mag. Lett. **85**, 513 (2005).
[33] X. K. Xi, D. Q. Zhao, M. X. Pan, W. H. Wang, Y. Wu, and J. J. Lewandowski, Phys. Rev. Lett. **94**, 125510 (2005).
[34] C. A. Schuh, and T. G. Nieh Acta Mater. **51**, 87 (2003).
[35] V. Keryvin, R. Crosnier, R. Laniel, V. H. Hoang, and J.-C. Sangleboeuf, J. Phys. D **41**, 074029 (2008).
[36] J. J. Lewandowski and A. L. Greer, Nature Mater. **5**, 15 (2006).
[37] A. A. Kundig, M. Ohnuma, D. H. Ping, T. Ohkubo, and K. Hono, Acta Mater. **52**, 2441 (2004).